IEEE Photonics Journal
An IEEE Photonics Society Publication

Open Access

Three-Layer Grating With the Enhanced Efficiency and Angular Bandwidth

Volume 9, Number 1, February 2017

Hongtao Li
Bo Wang

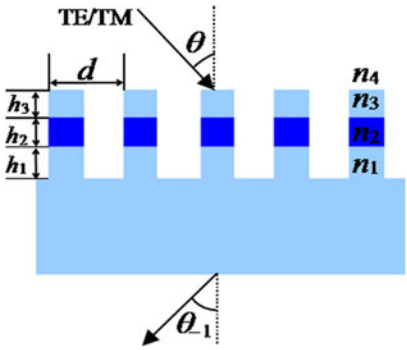

DOI: 10.1109/JPHOT.2017.2653622
1943-0655 © 2017 IEEE

Three-Layer Grating With the Enhanced Efficiency and Angular Bandwidth

Hongtao Li and Bo Wang

School of Physics and Optoelectronic Engineering, Guangdong University of Technology, Guangzhou 510006, China

DOI:10.1109/JPHOT.2017.2653622

Manuscript received December 5, 2016; revised January 9, 2017; accepted January 11, 2017. Date of publication January 16, 2017; date of current version February 1, 2017. This work was supported in part by the National Natural Science Foundation of China under Grant 11304044, in part by the Excellent Young Teachers Program of Higher Education of Guangdong Province, and in part by the Pearl River Nova Program of Guangzhou under Grant 201506010008. Corresponding author: B. Wang (e-mail: wangb_wsx@yeah.net).

Abstract: We theoretically and numerically analyze and design a three-layer rectangular-groove dielectric grating based on modal design and rigorous numerical calculation. This three-layer grating device can only diffract the transverse electric (TE)- or transverse magnetic (TM)-polarized plane light in the first diffractive order with high efficiency. By use of modal design, three thicknesses of the three grating layers can be sketchily calculated based on physical theory of two-beam interference with the chosen duty cycle of 0.6 and period of 610 nm for an operating wavelength of 800 nm under Littrow appliance. In order to obtain three exact thicknesses of the grating layers, a rigorous vector coupled-wave analysis method based on the Maxwell's theory is used to numerically calculate the high diffraction efficiencies of 99.0% and 97.7% in the first order for TE and TM polarizations, respectively. Moreover, a wide spectral width of 67 nm and a broad angular width of 10.88° can be shown.

Index Terms: Three-layer grating, high efficiency, broadband.

1. Introduction

All-dielectric diffractive gratings with periodic microstructure are made up of all dielectric materials. In today's numerous practical microsystems, all-dielectric diffractive gratings have some potential merits applied in Fabry-Pérot filters [1], biomimetic metasurfaces [2], optical metrology or imaging [3], multi-functional and multiwavelength metasurface devices [4], and frequencies for high-power applications [5]. In the great majority of reported research achievements, single-layer all-dielectric gratings [6]–[10] and two-layer all-dielectric gratings [11], [12] were largely investigated and they could be employed to achieve the high efficiency only in the –1st diffraction order with the broad spectral and angular bandwidths based on Littrow incident condition. In order to investigate a single-layer rectangular-groove all-dielectric grating from the reported studies, Clausnitzer *et al.* used the fused-silica transmission highly-efficient grating in the chirped-pulse amplification systems, their design results showed that the obtained maximum diffraction efficiency was 97% with an optimal groove depth 1.54 μm and a duty cycle of 0.45 for transverse electric (TE) polarization [6]. For studying a two-layer rectangular-groove all-dielectric grating, Shiozaki *et al.* designed a two-layer transmission grating with the maximum efficiency reaching 96.6% [11]. In particular, a single-layer blazed grating can also diffract an incident planewave in the 1st diffractive order with high efficiency

[13]. With the development of the multilayer gratings, three-layer gratings were reported [14], [15]. Guan *et al.* reported a high-performance metal/multilayer-dielectric trapezoidal-groove reflection grating with broad bandwidth, high efficiency of 99% in the –1st order for TE polarization and large fabrication tolerances. The designed grating ridge includes three dielectric layers, where the ridge consists of an HfO_2 in a center layer sandwiched between two SiO_2 layers [14]. In addition, the reported three-layer reflection grating was successfully fabricated by use of reactive ion beam etching method [16]–[18]. By using the fabricated three-layer reflection trapezoidal-groove grating in practical measurement, the measured relative spectral results were in good agreement with the simulation results by use of rigorous coupled-wave analysis (RCWA) method [19]. In order to observe the more details in fabricating the three-layer reflection trapezoidal-groove grating, Chen *et al.* provided the whole fabrication procedure and experimental results [15]. The fabrication procedure includes two experimental methods, which can be called photoresist mask method and ion-beam etching method. Based on the photoresist mask method, the spinner and oxygen plasma are used together to develop and mask etch the photoresist mask grating, respectively based on the appropriate development time, temperature and exposure condition. On account of ion-beam etching, in the RIBE system, the proposed three-layer grating was formed based on the special reactive gas, operating parameters and voltages of beam and accelerator. However, no one reports and proposes a three-layer all-dielectric rectangular-groove transmission grating. Furthermore, the two designed methods in this paper are RCWA method based on numerical optimization and modal method [20]–[23] based on the physical interpretation and evaluation.

In this paper, we firstly propose and design a three-layer all-dielectric rectangular-groove transmissive grating based on the modal design and RCWA method. In this design, we use two methods to design a novel three-layer rectangular-groove transmission high-efficiency diffraction optical grating, which are modal method and RCWA method. Based on the modal method, we can estimate the three thicknesses of layers and the propagating beam-interference mechanism can be well explained. Based on RCWA method, we can obtain the precise grating thicknesses. However, RCWA method is merely dependent on numerous numerical calculations based on Maxwell's numerical vector approach. In addition, it can not explain the whole coupling physical mechanism in the grating region. Therefore, based on modal method, the integrated physical coupled principle can be shown and we can confirm the rough scope of grating thicknesses, where the coupled efficiency in the –1st order can reach maximum value based on the coupled equations. On account of modal design, the three thickness of three layers are calculated and evaluated with the chosen duty cycle of 0.6 and period of 610 nm for an operating wavelength of 800 nm. On account of optimizing calculation, the exact thicknesses of layers are obtained with the optimal grating parameters. The optimum results of the diffraction efficiencies in the –1st order for two polarizations can be enhanced compared to the designed single-layer all-dielectric rectangular-groove grating [6] and two-layer all-dielectric rectangular-groove grating [11]. Moreover, the investigated angular bandwidth of 10.88° is also enhanced compared to the sandwiched two-layer all-dielectric rectangular-groove grating [12].

In this paper, we have introduced the detailed fabrication processes of three-layer trapezoidal-groove reflective gratings based on photoresist mask method and ion beam etching method. In [14], Guan *et al.* used the RCWA method to design a three-layer trapezoidal-groove reflective grating, based on the numerical designed parameters, the experimental measured diffraction efficiencies can be in agreement with the calculated diffraction efficiencies based on numerical optimization. Therefore, one can see that the numerical RCWA method is a feasible accurate method for designing our three-layer grating. However, there are some differences between our design and the previous proposed designs. Firstly, in previous structures, shape of the proposed three-layer grating grooves are trapezoid, in our structure, shape of the three-layer grating groove is rectangle. Secondly, previous work was merely focused on numerical design, in our work, we can employ a theoretical approach to analyze the coupling phenomenon and predict the three thicknesses of layers. Based on theoretical prediction, the RCWA method is used to confirm the exact thicknesses. In addition, A RCWA code is used. Values of numerical parameters (as the number of Rayleigh harmonics) are 80 and the numerical results have achieved convergence. For manufacturing such the grating configuration, the used methods are photoresist mask method and ion-beam etching method, the

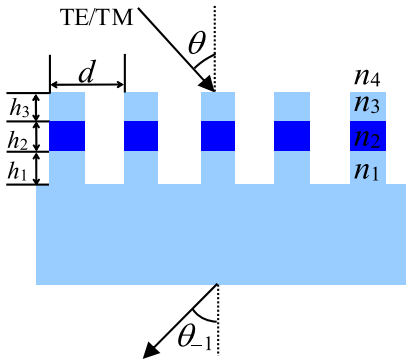

Fig. 1. Monoperiodic three-layer rectangular-groove dielectric grating structural diagram.

fabrication details are similar to the reported details in [15]. In our paper, we use the rectangular-groove grating to realize a high-efficiency wideband optical device. The device can be fabricated by using photoresist mask technique and ion-beam etching technique. In fact, the rectangular-groove grating with a relative vertical wall can be realized. In the most reported papers, the gratings with rectangular-groove structure are largely investigated and the gratings can be successfully fabricated by using conventional photoresist mask method and ion-beam etching method [6], [7]. Similarly, by using photoresist mask method and ion-beam etching method, the relative complex fabrication procedures can be used to fabricate three-layer rectangular-groove grating compared to the single-layer gratings. Therefore, the rectangular-groove three-layer grating with a relative vertical wall can be fabricated.

2. Modal Design and Optimizing Calculation

Monoperiodic three-layer rectangular-groove dielectric grating structural diagram can be exhibited in Fig. 1. As can be seen from Fig. 1, the grating rectangular ridge can be comprised of two different dielectric materials with three different etching depths, where the two dielectric materials are fused silica with the refractive index of $n_3 = 1.45$ and $n_1 = 1.45$ and Ta_2O_5 with the refractive index of $n_2 = 2.0$. In the grating geometrical parameters, the three thicknesses of three grating layers are h_1, h_2 and h_3. In addition, three-layer grating period indicates for d and the duty cycle is defined by ratio of ridge width to period. Under the Littrow appliance, a plane polarized light with a working wavelength of λ incidents from the air with the refractive index of $n_4 = 1.0$ on the three-layer grating and the incident Bragg angle is θ and the angular related expression is that of $\theta = \sin^{-1}(\lambda/(2d))$.

Based on a theoretical modal method, the two-beam interference theory can expressly explain coupled mechanism in the three-layer transmissive grating. When the incident wave propagates in the grating, the two grating modes are stimulated, every grating mode has the nearly identical energy from the incident wave. The ability of energy exchanging can be determined by the overlap integral, and the excited two grating modes have the uniform spatial frequency and have the same sinusoidal propagating form with the incident wave [23]. Based on the modal design, the only two excited mode 0 and mode 1 can diffuse in the grating layers for TE and transverse magnetic (TM) polarizations. Because of the asymmetry between the two modes, effective indices in the mode 0 and mode 1 are different. Based on the modal analysis in this paper, the excited mode 0 and mode 1 are called the Bloch modes of the grating [24]. Besides, the all properties (effective indices) of modes propagating in the grating could be obtained with an appropriate RCWA code. Even more important, the effective index difference between the mode 0 and mode 1 can contribute to the coupling efficiency in the –1st order. Therefore, the calculated effective indices from the proper function can be described as [21]

$$F\left(n_{eff}^2\right) = \cos\left(\frac{2\pi d \sin\theta}{\lambda}\right). \tag{1}$$

For TE polarization

$$F\left(n_{eff}^2\right) = \cos\alpha\cos\beta - \frac{1}{2}\varepsilon\sin\alpha\sin\beta \tag{2}$$

where $\alpha = \frac{2\pi(1-f)d\sqrt{n_g^2-n_{eff}^2}}{\lambda}$, $\beta = \frac{2\pi fd\sqrt{n_r^2-n_{eff}^2}}{\lambda}$, $\varepsilon = \frac{(1-f)\beta}{f\alpha} + \frac{f\alpha}{(1-f)\beta}$.

For TM polarization

$$F\left(n_{eff}^2\right) = \cos\alpha\cos\beta - \frac{1}{2}\xi\sin\alpha\sin\beta \tag{3}$$

where

$$\xi = \frac{f\alpha n_r^2}{(1-f)\beta n_g^2} + \frac{(1-f)\beta n_g^2}{f\alpha n_r^2} \tag{4}$$

where n_r and n_g mean the refractive indices of the grating ridge and grating groove, respectively. Equations (1) to (4) express the grating dispersion conditions, which are determined by some of the grating parameters. According to simultaneous (1) to (4), the grating effective indices are obtained. The four equations are deduced from modal theory of waveguides. In layer 1, n_r is 1.45 and n_g is 1.0. In layer 2, n_r is equal to 2.0 and n_g is equal to 1.0. In layer 3, n_r and n_g are 1.45 and 1.0, respectively. Effective indices are obtained by simultaneous (1) to (4). Under the Littrow condition, the $F(n_{eff}^2)$ is equal to -1 in eq. (1). Due to the duty cycle of f and period of d are given in this paper, the effective indices in each layer can be calculated with the different refractive index of grating groove of n_r by simultaneous (2) to (4). For TE and TM polarizations, effective indices in the three layers are displayed as: $n_{0eff}^{1TE} = 1.2575$, $n_{1eff}^{1TE} = 0.9804$, $n_{0eff}^{2TE} = 1.8368$, $n_{1eff}^{2TE} = 1.4058$, $n_{0eff}^{3TE} = 1.2575$, $n_{1eff}^{3TE} = 0.9804$, $n_{0eff}^{1TM} = 1.1693$, $n_{1eff}^{1TM} = 0.9880$, $n_{0eff}^{2TM} = 1.7390$, $n_{1eff}^{2TM} = 1.1943$, $n_{0eff}^{3TM} = 1.1693$, and $n_{1eff}^{3TM} = 0.9880$.

At the bottom of the grating ridge, the phase difference can be formed due to the interference effect. The accumulated phase difference can influence on the ultimate coupled efficiency. In theory, the accumulated phase difference in three layers should satisfy the odd-numbered multiples of π, efficiency in the –1st diffractive order can attain the nearly 100% result. Thus, the related expression is obtained [23]:

$$\eta_{-1st} = \sin^2\left(\frac{\Delta\varphi}{2}\right) \tag{5}$$

where the $\Delta\varphi$ shows that of the phase difference. The equation can meet for both TE and TM polarizations simultaneously. Hence, the relative expressions for two polarizations in three layers are

$$\Delta\varphi^{TE} = \frac{2\pi}{\lambda}\left[\left(n_{0eff}^{1TE} - n_{1eff}^{1TE}\right)h_1 + \left(n_{0eff}^{2TE} - n_{1eff}^{2TE}\right)h_2 + \left(n_{0eff}^{3TE} - n_{1eff}^{3TE}\right)h_3\right] = (2p+1)\pi \tag{6}$$

and

$$\Delta\varphi^{TM} = \frac{2\pi}{\lambda}\left[\left(n_{0eff}^{1TM} - n_{1eff}^{1TM}\right)h_1 + \left(n_{0eff}^{2TM} - n_{1eff}^{2TM}\right)h_2 + \left(n_{0eff}^{3TM} - n_{1eff}^{3TM}\right)h_3\right] = (2q+1)\pi \tag{7}$$

with p and q are arbitrary integers. Equations (5) to (7) express the interference effect between the coupled modes. After the two different grating modes with different propagating constants pass through the grating ridge with three different thicknesses, the phase differences are formed. The coupled efficiency can be dependent on the phase difference. Furthermore, the three equations are deduced from modal method of waveguides. Fig. 2 shows the four different lines of highly efficient for TE and TM polarizations on account of (6) and (7) for a duty cycle of 0.6 under an operating wavelength of 800 nm. In Fig. 2, we presume that the thickness of h_3 is equal to 0.1 μm, integer of 0 illustrates that the accumulation of phase difference is about π with the different thicknesses of h_1 and h_2, integer of 1 demonstrates the cumulative phase difference can come to 3π versus the different h_1 and h_2. There are two intersections between the red line and the green line and between the blue line and the black line. The intersections show two polarization-independent grating devices with duty cycle of 0.6 and

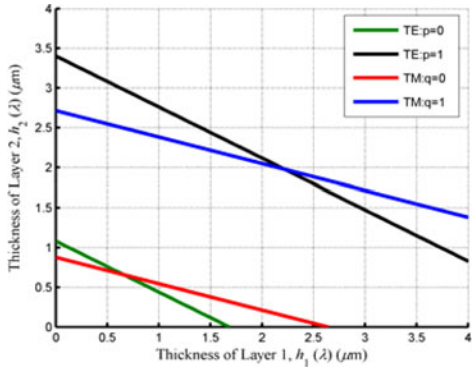

Fig. 2. Four different lines of highly efficient for TE and TM polarizations on account of (6) and (7) for a duty cycle of 0.6 under an operating wavelength of 800 nm.

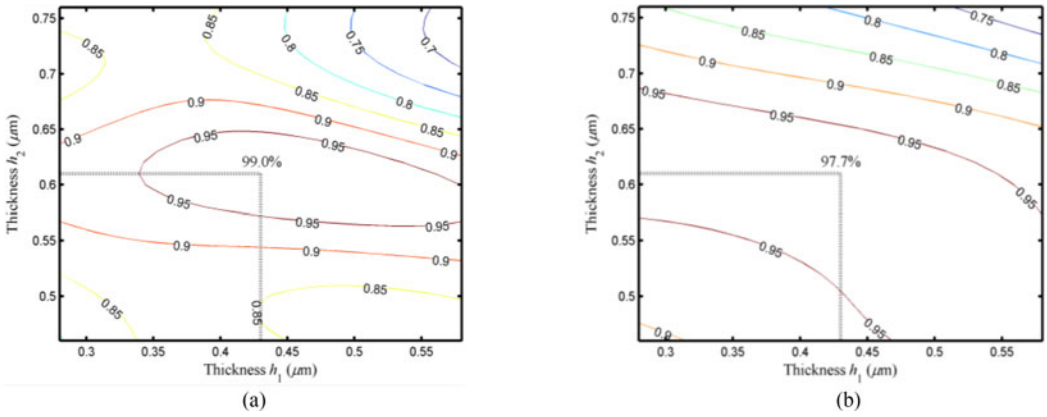

Fig. 3. Etching thicknesses of h_1 and h_2 versus the transmissive efficiency with the optimum h_3, duty cycle and period under Littrow appliance for two polarizations. (a) TE polarization. (b) TM polarization.

period of 610 nm, in order to facilitate fabricating technology, the only one intersection between the red line and the green line needs to be considered. Therefore, an optimum polarization-independent device is obtained with the $h_1 = 0.6559\lambda = 0.52472\,\mu$m and $h_2 = 0.6580\lambda = 0.52640\,\mu$m. In this paper, we give the approximate layer thicknesses obtained with the approximate method with a precision of a fraction of 1 angstrom. In practical grating fabrication progress, the thickness of grating layer with small micron order can meet numerous advanced precision optical instruments and equipment.

Based on modal design, theoretically estimated grating thicknesses of h_1, h_2 and h_3 are 0.52472 μm, 0.52640 μm and 0.10 μm, respectively. Although the obtained results are not exact at all, the results should be in close proximity to the accurate ones. Fig. 3 shows the etching thicknesses of h_1 and h_2 versus the transmissive efficiency with the optimum h_3 of 0.1 μm, duty cycle of 0.6 and period of 610 nm under Littrow appliance. In Fig. 3, three-layer grating can diffract the TE polarization in the –1st diffractive order with a high efficiency of 99.0%, where the optimum thicknesses of h_1 and h_2 are 0.43 μm and 0.61 μm, respectively. For a TM polarization, transmissive efficiency in the –1st order can achieve 97.7% for an operating wavelength of 800 nm and duty cycle of 0.6 with optimum thicknesses of 0.43 μm, 0.61 μm and 0.1 μm. In our design, the difference between the two first thicknesses is very small. In order to ensure the fabrication processes with enough accuracy, the fabrication tolerance for the first two thicknesses are needed for investigating. In Fig. 3, the transmission efficiencies more than 95% in the minus-first order with 0.34 μm $< h_1 <$ 0.58 μm and 0.57 μm $< h_2 <$ 0.64 μm for both TE and TM polarizations with a polarization-independent property.

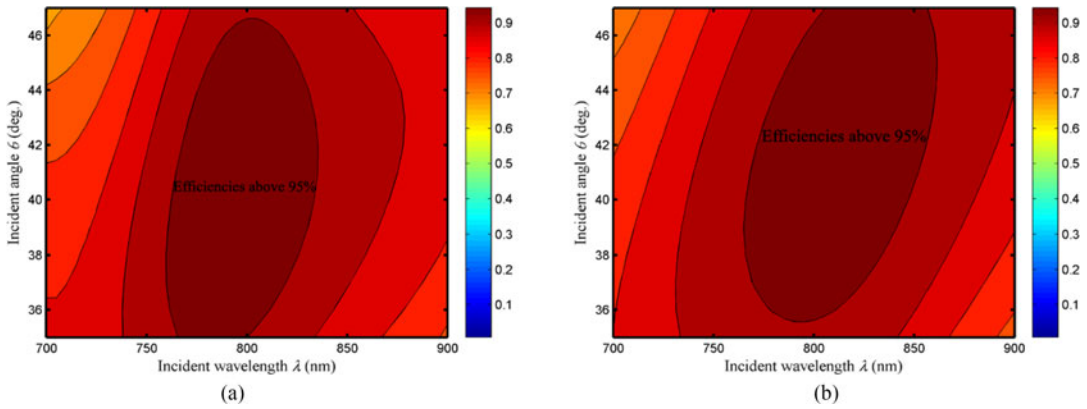

Fig. 4. Transmissive efficiency versus incident wavelength and angle at a duty cycle of 0.6 with three optimal grating thicknesses for two polarizations. (a) TE polarization. (b) TM polarization.

3. Research on the Applicable Broad Working Bandwidths for Three-Layer Grating

Fig. 4 shows transmissive efficiency versus incident wavelength of λ and incident angle at a duty cycle of 0.6 with three optimal grating thicknesses for TE and TM polarizations. As can be shown from Fig. 4, with the different wavelengths, the transmissive efficiencies in the 0th order and the –1st order are different. This three-layer dielectric grating can diffract into the –1st order with diffractive efficiencies over than 80%, where the incident wavelength coverage can be changed from the 700 nm to the 900 nm. At the central wavelength of 800 nm, the optimum three-layer grating is obtained with the optimal thicknesses of layers for TE and TM polarizations. Around the central wavelength of 800 nm, efficiencies are more than 95% in the –1st order in wavelength bandwidth range of 766–833 nm for TE and TM polarizations. In Fig. 4, one can see that transmissive efficiencies are greater than 95% in the –1st order for TE polarization over an incident angular bandwidth range of 35.01°–46.63°. In the broad incident angular bandwidth ranged from 35.60° to 46.48°, transmissive efficiencies lager than 95% are obtained for a TM polarization. In Fig. 4, efficiencies above 95% have depicted with the very broad color scale. Furthermore, the regions of interest in Fig. 4 are shown as the darkest red. In the grating design, the influences of refractive index of dielectric layers on the optical spectral response and angular dependent response of the grating are important performances, which should be taken into consideration. In our design, we design a dielectric multilayer grating, where the grating groove layer can be composed two dielectric materials with two different refractive indices. According to observe the proper function, the diffractive beam can propagate in the different materials with different effective indices for TE and TM polarizations. One can see that once the effective indices are changed, the phase differences can be influenced. In addition, the obtained theoretical coupled efficiencies based on modal method can control the grating spectral bandwidth and angular bandwidth.

4. Conclusion

In conclusion, a three-layer all-dielectric rectangular-groove transmissive grating is designed. For evaluating the three thicknesses of three layers, modal method is used, and we obtain the three thicknesses of 0.52472 μm, 0.52640 μm and 0.1 μm. In our design, the theoretical estimation based on modal method is a very good approximation to the exact values obtained using RCWA. Modal method is a theoretical method, which can only evaluate and forecast the exact grating parameters. Therefore, the error is inevitable, where the error is around 20% in this design. According to investigate our three-layer grating diffraction performance, the incident angular bandwidth of 10.88° is enhanced compared to the reported angular bandwidth of 7.2° [12]. In addition, the diffraction

efficiency in the minus-first order for TE polarization is enhanced compared to the single-layer grating [6] and the two-layer grating [11]. Therefore, our designed three-layer rectangular-groove transmissive high-efficiency broadband grating device should be a novel diffractive optical component, which can provide the new design approach for future good-performance diffractive multilayer gratings.

References

[1] W. Wang, X. Gao, X. Fang, X. Li, H. Zhu, and Y. Wang, "Transmission properties of Fabry-Pérot filter consisting of silicon-based high-contrast gratings," *IEEE Photon. J.*, vol. 8, no. 1, Feb. 2016, Art. no. 6800614.

[2] S. Jahani and Z. Jacob, "All-dielectric metamaterials," *Nature Nanotechnol.*, vol. 11, pp. 23–36, 2016.

[3] S. Zhou, Y. Yang, S. Hu, and X. Xu, "Scalar-based analysis of phase gratings etched in the micro/nanofabrication process," *IEEE Photon. J.*, vol. 7, no. 4, Aug. 2015, Art. no. 4900111.

[4] E. Arbabi, A. Arbabi, S. M. Kamali, Y. Horie, and A. Faraon, "Multiwavelength metasurfaces through spatial multiplexing," *Sci. Rep.*, vol. 6, 2016, Art. no. 32803.

[5] L. Li *et al.*, "Reconfiguration all-dielectric metamaterial frequency selective surface based on high-permittivity ceramics," *Sci. Rep.*, vol. 6, 2016, Art. no. 24178.

[6] T. Clausnitzer *et al.*, "Highly efficient transmission gratings in fused silica for chirped-pulse amplification systems," *Appl. Opt.*, vol. 42, pp. 6934–6938, 2003.

[7] H. Cao, C. Zhou, J. Feng, P. Lu, and J. Ma, "Design and fabrication of a polarization-independent wideband transmission fused-silica grating," *Appl. Opt.*, vol. 49, pp. 4108–4112, 2010.

[8] S. Pi *et al.*, "Dielectric-grating-coupled surface plasmon resonance from the back side of the metal film for ultrasensitive sensing," *IEEE Photon. J.*, vol. 8, no. 1, Feb. 2016, Art. no. 4800207.

[9] K. Ito and H. Iizuka, "Highly efficient 1st-order reflection in Littrow mounted dielectric double-groove grating," *AIP Adv.*, vol. 3, 2013, Art. no. 062119.

[10] Y. Li, J. Deng, J. Li, and Z. Li, "Sensitive orbital angular momentum (OAM) monitoring by using gradually changing-period phase grating in OAM-multiplexing optical communication systems," *IEEE Photon. J.*, vol. 8, no. 2, Apr. 2016, Art. no. 7902306.

[11] M. Shiozaki and M. Shigehara, "Novel design of polarization independent multi-layer diffraction grating with high angular dispersion," *SEI Tech. Rev.*, vol. 59, pp. 27–31, 2005.

[12] B. Wang, W. Shu, L. Chen, L. Lei, and J. Zhou, "Reflection-reduced two-layer grating with nearly 100% diffraction efficiency," *IEEE Photon. Technol. Lett.*, vol. 26, no. 5, pp. 501–503, Mar. 2014.

[13] T. Shiono, T. Hamamoto, and K. Takahara, "High-efficiency blazed diffractive optical elements for the violet wavelength fabricated by electron-beam lithography," *Appl. Opt.*, vol. 41, pp. 2390–2393, 2002.

[14] H. Guan *et al.*, "High-efficiency, broad-bandwidth metal/multilayerdielectric gratings," *Opt. Lett.*, vol. 39, pp. 170–173, 2014.

[15] H. Chen, H. Guan, L. Zeng, and Y. Jin, "Fabrication of broadband, high-efficiency, metal-multilayer-dielectric gratings," *Opt. Commun.*, vol. 329, pp. 103–108, 2014.

[16] M. Ma *et al.*, "Polarized light emission from GaInN light-emitting diodes embedded with subwavelength aluminum wire-grid polarizers," *Appl. Phys. Lett.*, vol. 101, 2012, Art. no. 061103.

[17] M. R. Saleem *et al.*, "Replicable one-dimensional non-polarizing guided mode resonance gratings under normal incidence," *Opt. Exp.*, vol. 20, pp. 16974–16980, 2012.

[18] T. Kämpfe, S. Tonchev, G. Gomard, C. Seassal, and O. Parriaux, "Hydrogenated amorphous silicon microstructuring for 0th-order polarization elements at 1.01.1 mu m wavelength," *IEEE Photon. J.*, vol. 3, no. 6, pp. 1142–1148, Dec. 2011.

[19] M. G. Moharam, D. A. Pommet, E. B. Grann, and T. K. Gaylord, "Stable implementation of the rigorous coupled-wave analysis for surface-relief gratings: Enhanced transmittance matrix approach," *J. Opt. Soc. Amer. A.*, vol. 12, pp. 1077–1086, 1995.

[20] I. C. Botten, M. S. Craig, R. C. Mcphedran, J. L. Adams, and J. R. Andrewartha, "The dielectric lamellar diffraction grating," *Opt. Acta*, vol. 28, pp. 413–428, 1981.

[21] T. Clausnitzer *et al.*, "An intelligible explanation of highly-efficient diffraction in deep dielectric rectangular transmission gratings," *Opt. Exp.*, vol. 13, pp. 10448–10456, 2005.

[22] F. Yang and Y. Li, "Evaluation and improvement of simplified modal method for designing dielectric gratings," *Opt. Exp.*, vol. 23, pp. 31342–31356, 2015.

[23] T. Clausnitzer, T. Kämpfe, E.-B. Kley, A. Tünnermann, A. V. Tishchenko, and O. Parriaux, "Investigation of the polarization-dependent diffraction of deep dielectric rectangular transmission gratings illuminated in Littrow mounting," *Appl. Opt.*, vol. 46, pp. 819–826, 2007.

[24] T. Matsui *et al.*, "Experimental investigation of double-groove grating satisfying total internal reflection condition," *Opt. Exp.*, vol. 22, pp. 25362–25370, 2014.